International Journal of Physical Sciences Vol. 7(9), pp. 1346 - 1352, 23 February, 2012
Available online at http://www.academicjournals.org/IJPS
DOI: 10.5897/IJPS11.1711
ISSN 1992 - 1950 ©2012 Academic Journals

Full Length Research Paper

Finite element method for simulation of Tsunami run-up from QuikiBird satellite data

Maged Marghany

Institute of Geospatial Science and Technology (INSTEG), Universiti Teknologi Malaysia 81310 UTM, Skudai, Johor Bahru, Malaysia. E-mail: maged@utm.my or magedupm@hotmail.com.

Accepted 09 February, 2012

In this paper, work was carried out to simulate three-dimensional (3-D) tsunami run-up from high resolution remote sensing satellite data of QuickBird. In doing so, the tsunami wave spectra are extracted from QuickBird data using two dimensional di Fourier transform (2-DFFT). The tsunami propagation equation was then solved based on the standard Galerkin finite element approach to simulate 3-D tsunmai run-up. The results of this study have shown that the integration between different mathematical and numerical models is providing accurate 3-D reconstruction and simulation for tsunami run-up.

Key words: QuickBird satellite data, tsunami run-up, 2-DFFT, 3-D reconstruction, finite element method, Galerkin finite element.

INTRODUCTION

Mathematical model plays tremendous roles in understanding the mechanism generation of environmental disasters. Standard numerical model is requested for forecasting and predicting long-term of disaster occurrences. Consequently, an accurate numerical model can assist the decision makers in establishing perfect networking early warning systems to prevent disaster impacts on the surrounding environment. One of tremendous disaster is the earthquake off the Sumatra coast on 26th December 2004.

Consistent with Paris et al. (2007), at 00:58:53 UTC on Sunday, 26th December, 2004, the 2004 Indian Ocean earthquake occurred because of an undersea megathrust earthquake with an epicentre off the west coast of Sumatra, Indonesia. The hypocentre of the core earthquake was about 160 km (100 mi). in the Indian Ocean just north of Simeulue island, off the western coast of northern Sumatra. It was at a depth of 30 in the northern section of the Sunda megathrust (Nalbant et al., 2005). Marghany and Suffian (2005) stated that, the Indian Ocean tsunami is powerful releasing energy of approximately 20 x 1017 Joules, or 475,000 kilotons (475 megatons), or the equivalent of 23,000 Hiroshima bombs. Furthermore, the 26th December 2004 tsunami traveled 600 km in 75 min, which means it reached a speed of 480 km/h. In addition, Lovholt et al. (2006) stated that splay faults, or secondary "pop up faults", caused long, narrow parts of the sea floor to pop up in seconds. This quickly raised up the height and increased the speed of waves, causing the complete destruction of the nearby Indonesian town of Lhoknga (Sibuet et al., 2007).

There is no doubt that these walls of water were capable of inflicting massive damages along the coastal lands. The consequent tsunami devastated coastlines around the ocean and killed around 226,000 people, with millions left destitute. The tsunami traveled both east and west away from the fault line, which runs north-south. This is why nearby countries to the North such as low-lying Bangladesh, escaped unscathed, while several more distant countries to the West such as Somalia, suffered considerable damage (Marghany and Suffian, 2005). Nevertheless, satellite remote sensing data could not work as warning alarm to prevent the occurrences of the disaster.

Walter et al. (2005) stated that, theoretically, sea level anomalies observed by altimetry should reflect tsunami waves. Conversely, observation is difficult, since the additional height is one of the signals of ocean variability. In this regards, scientists just used remote sensing tool to identify the tsunami’s impact zones (Oo et al., 2005; Marghany and Suffian, 2005; Salinas et al., 2006; Kouchi and Yamazaki, 2007; Ibarhim et al., 2009).

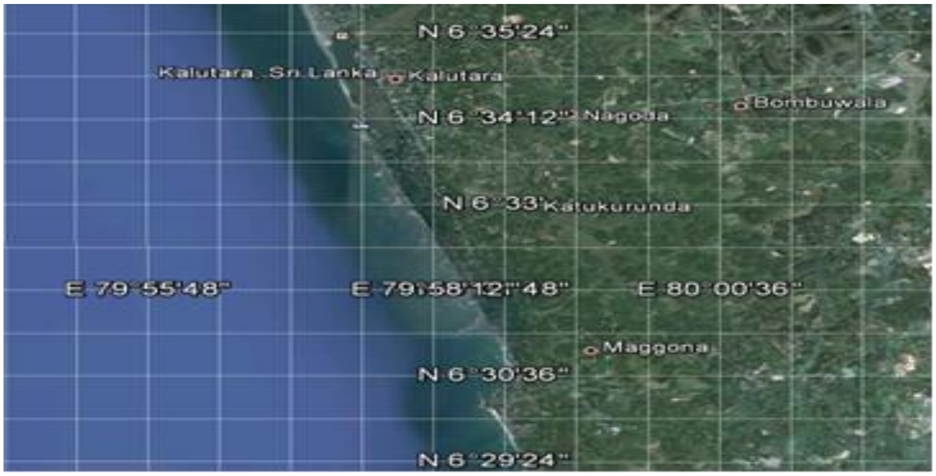

Figure 1. Geographical location of study area.

Kouchi and Yamazaki (2007) have implemented the normalized difference vegetation index (NDVI), soil index (NDSI) and water index (NDWI) to detect tsunami-inundated areas from ASTER images. Further, they employed shuttle radar topography mission (SRTM) data to perform geomorphological classification and to determine the extent of tsunami run-up. Consequently, they reported that most pixels with normalized difference vegetation index (NDVI) decreased subsequently when the tsunami occurred in the low plain areas.

Ibrahim et al. (2009) have used SPOT-5 satellite data to determine the rate of land changes due to tsunami for Kuala Muda, Kedah, Malaysia. Further, they improved digital elevation models (DEM) using texture layers by integration with Brovey transformed band and maximum likelihood classifier. Therefore, Ibrahim et al. (2009) reported that the SPOT-5 moderate resolution sensor was reliable in identifying land damages due to tsunami. Nevertheless, the above studies were based on conventional methods of generating DEM that caused high level of uncertainties. Walter et al. (2005) stated that, theoretically, sea level anomalies observed by altimetry should reflect tsunami waves. Conversely, observation is difficult, since the additional height is one of the signals of ocean variability.

There are few studies that have concerned for the simulation of tsunami run-up from remote sensing data. Marghany and Mazlan (2011) stated that, run-up model is required several parameters' such as frequency, wavelength and wave height, and the beach slope. In addition, run-up model is required to accurate DEMs of coastal zones. Salinas et al. (2006) conversely stated that, to approach the run–up and inundation problem, the non–linear shallow water equations must be solved with an appropriate treatment for breaking waves and moving shore lines. Likewise, they have reported that the complex geometry of the coastal line coupled with arbitrary beach and sea floor profiles, makes solving the shallow water equations a formidable task which only can be approached numerically (Salinas et al., 2006). Under this circumstance, the standard methods are required to acquire accurate successive tsunami wave propagation from satellite imagery, and to avoid uncertainty might arise due to absence of real time *in-situ* measurements.

In this paper, we address the question of modelling tsunami run-up using remote sensing data without the need to include any *in-situ* measurement data. Certainly, there was no wave data collected during the disaster event on 26th December, 2004 (Walter et al., 2005). Two hypothesis examined are:(i) the QuickBird satellite data can be used to detect tsunami wave spectra; and (ii) finite element scheme of Galerkin method can be integrate with tsunami spectra information to reconstruct 3-D tsunami run-up.

METHODOLOGY

Study area

The study area is chosen along the Kalutara coastline. Kalutara is a resort town located approximately 40 km south of Colombo in Sri Lanka. The coastline is planted by coconut trees. Further, the 38 m long Kalutara Bridge was built at the mouth of the Kalu Ganga River and serves as a major link between the country's western. Kalutara district is a district in Western Province, Sri Lanka. Its area is 1,606 km². The district was hit by the tsunami generated by the 2004 Indian Ocean earthquake. This area is suited between 6° 30′ 36″ N to 6° 35′ 24″ and 79° 55′ 48″ E to 80° 00′ 36″ E. The coastline is dominated by muddy sediment due to the existence of several rivers such as Kalu Ganga River (Figure 1).

The coastal zone is dominated by DEM that is ranged between 5 to 13 m above the sea level. The main feature and of this coastal zone is existence of the high sand dunes. They are scattered along stretches of the southeast the far northeast coast were very effective in with standing the tsunami wave (Stein and Okal, 2005 and Joe et al., 2012).

Figure 2. The multispectral QuickBird satellite is used in this study.

Satellite data

The multispectral QuickBird satellite data within less than 1 m pixel resolution is chosen. For ocean wave spectra extraction the composite colour bands of 450 to 520 nm (blue), 520 to 600 nm (green) and 630 to 690 nm (red) was used (Figure 2). The multispectral QuickBird satellite shows a portion of the Southwest coast of Sri Lanka, near Kalutara and was taken on Sunday December 26, 2004, at 10:20 a.m. local time, slightly less than four hours after the 6:28 a.m. (local Sri Lanka time) earthquake and shortly after the moment of tsunami impact (Marghany and Suffian, 2005; Marghany and Mazlan, 2011).

3-D MODEL FOR TSUNAMI RUN-UP ESTIMATION

The satellite QuickBird data was used to extract the information on tsunami wave spectra using 2-D Fourier transform (FFT). To estimate the tsunami run-up, the finite element model is used.

Wave spectra estimation from QuickBird satellite data

Since the wave changes its direction and wavelength as it propagates, the two dimensional (2-D) discrete Fourier transform (DFT) was used to derive the wave number spectra from QuickBird satellite data. First, choose a window kernel size of 512 × 512 pixels and lines with the pixel size equal to ΔX. In fact, it is impossible to acquire wave spectra parameters by using kernel window size less than 512 x 512 pixels and lines. According to Populus et al. (1990), 2-DFFT transfers the 2-D QuickBird satellite data into frequency spectra domain $(k_x \text{ and } k_y)$. The frequency spectra domain is used to estimate the variation of wavelength variation, along with the spectra frequency domain, as wavelength inversely proportional to the frequency domain.

Following Populus et al. (1990), Marghany (2001) and Marghany and Mazlan (2011), let $X(m_1, m_2)$ represent the digital count of the pixel at (m_1, m_2) which is used to perform DFT, which is given as

$$F(k_x, k_y) = N^{-2} \sum_{m_2=0}^{N-1} \left[\sum_{m_{11}=0}^{N-1} X(m_1, m_2).e^{-ik_x.m_1.\Delta X} \right] .e^{-ik_y.m_2.\Delta X} \tag{1}$$

where, $n_1 \text{ and } n_2 = 1, 2, 3, ..., N$ and k_x and k_y are the wave numbers in the *x* and *y* directions, respectively. Following Marghany et al. (2011), the Gaussian algorithm was applied to remove the

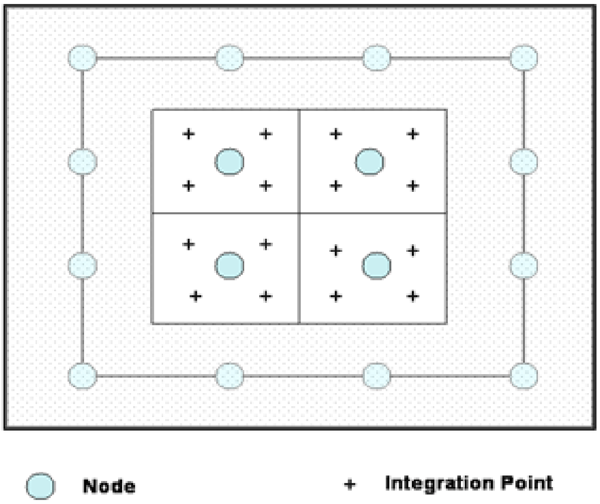

Figure 3. Finite element grid used in this study.

noise from the image and smooth the spectral peak into normal distribution curve. The wavelength was estimated by using autocorrelation algorithm. The autocorrelation algorithm was implemented in the mid row and the mid column. In a two dimensional wave number spectrum, the spectral peak (*C*) located at *X* and *Y* respectively, (C_x, C_y) of a *N x N* image spectrum which has the wavelength λ and the wave direction θ (Populus et al., 1990):

$$\lambda = \frac{\Delta x.lag(pixels)}{(k_x{}^2 + k_y{}^2)^{0.5}} \qquad (2)$$

$$\theta = \tan^{-1}(\frac{k_y}{k_x}) \qquad (3)$$

Then water elevation η caused by tsunami wave can be modelled using solitary wave. In this regards, solitary wave consists of a complex spectrum of frequencies which is uniquely described by the height-to-depth ratio ***H***=*H/d* where *H* is height and *d* is depth Gedik et al. (2005). The modelling of η is adopted using solitary wave model as follows:

$$\eta(x,0) = H\sec h^2(0.75H)^2(x - X_1) \qquad (4)$$

where x and X_1 are pixel locations of tsunami wave propagation in QuickBird satellite data. Where $x = X_1$ at in time t=0. The estimation of the tsunami hight *H* then can be done by using the formula adopted from Synolakis (1987) as follows:

$$\lambda = \frac{2d}{\sqrt{0.75H}} \arccos h \frac{1}{\sqrt{0.05}} \qquad (5)$$

Where λ is the wavelength extracted from QuickBird satellite data using Equation 2, *d* is the water depth that is acquired from USGS (2004) and ranged between 5 to 200 m along the coastal water of Sri-Lanka. The bathymetry information acquired directly from USGS (2004) site. Equation 5 is used to estimate tsunami wave height from QuickBird satellite data and then substituted in Equation 4 to calculate tsunami wave elvation η.

Numerical model of Tsunami run-up

In the coastal zone, the wavelength of the incident tsunami becomes shorter and the amplitude becomes larger as the leading of a tsunami propagate into shallower water (Goto and Ogawa, 1992). Therefore, in the Cartesian coordinate system the equation of tsunami wave propagation can be written as follows

$$\frac{\delta\eta}{\delta t} + \frac{\delta}{\delta x}(du) + \frac{\delta}{\delta}(dv) = 0 \qquad (6)$$

$$\frac{\delta u}{\delta t} + g\frac{\delta\eta}{\delta x} = 0 \qquad (7)$$

$$\frac{\delta v}{\delta t} + g\frac{\delta\eta}{\delta y} = 0 \qquad (8)$$

Where η is the tsunami elevation which has been estimated from the Equation 4 , *u* and *v* are the tsunami velocity components in the *x* and *y* directions, *g* is the gravity acceleration and *h* is the water depth which is obtained from USGS (2004).

Then, the run-up (*R*) is modelled using the equation adopted from Gedik et al. (2005)

$$\frac{R}{d} = 1.25\left(\frac{\pi}{2\beta}\right)^{0.2}\left(\frac{H}{d}\right)^{1.25}\left(\frac{H}{\lambda}\right)^{-0.15} \qquad (10)$$

Where β the inclination angle of the plane beach, λ is the wavelength is modelled from QuickBird satellite data using Equation 2, *d* is the water depth, and *H* is tsunami height is modelled using equation 5.

Galerkin finite element

In this study, a mesh-less method is applied because it does not require a time-consuming mesh generation for modelling the computational domain. The element-free Galerkin method (EFGM) proposed by Hiroshi et al. (1994), is one of the practical mesh-less method. Then, the EFGM is used to solve the shallow water wave equations. For the EFGM, state value of arbitrary evaluation points in the domain is solved by a kind of moving least square method (MLSM) from state value of nodal which exists in the circle of which the centre is the evaluation points. The radius of circle is called ‘domain of influence’, for introducing a weight function which increases the effect according to the distance between evaluation point and every node in the domain of influence to the MLSM (Figure 3).

Moving least-squares method (MLSM)

The moving least-squares (MLS) method can be used in function approximation. The so-called MLS method, which reconstructs the continuous function from an arbitrary set of particles via the calculation of a weighted least square (LS) around the evaluation point, is used to obtain the local approximate derivatives. The MLS is generally more accurate than the grid-based numerical methods near irregular surfaces (Singh, 2004). The unknown function, in MLSM is expressed as follows,

$$\phi^h(x) = \sum_j^N p_j(x) a_j(x) \equiv \{p(x)\}^T \{a(x)\} \quad (11)$$

Where p_j is linear basis including in the space coordinates, a_j is undetermined coefficient and *N* is number term used at expansion. For example, *p* is expressed as follows (Singh, 2004),

$$\{p(x,y,z)\}^T = \{1, x, y, z\} \qquad (N=4) \quad (12)$$

$$\{p(x,y,z)\}^T = \{1, x, y, z, x^2, xyz, y^2\} \qquad (N=7) \quad (13)$$

Following Cinegoski et al. (1988), Belyschko et al. (1994) and Singh (2004), the coefficient $a_j(x)$ is obtained by minimizing the performance function *J* as follows,

$$J = \sum_i^N w(x-x_i)\{\phi_i^h(x) - \phi_i\}^2 = \sum_i^N w(x-x_i)\{\{p(x)\}^T\{a(x)\} - \phi_i\}^T, \quad (14)$$

Where *N* is the number of nodes within neighborhood of *x* and x_i is the space coordinates of an arbitrary node x_i within neighborhood of *x*. $\sum_i^N w(x-x_i)$ is weighting function that depends on the distance between point *x* and node x_i. Finally, $\phi_i^T(x)$ is interpolation function and is defined as (Singh, 2004),

$$\phi_i^T(x) = \{p(x)\}^T [\sum_i^N w(x-x_i) p(x_i) p^T(x_i)]^{-1} [w(x-x_1) p(x_1),$$
$$w(x-x_2) p(x_1), \ldots\ldots\ldots, w(x-x_n) p(x_n)] \quad (15)$$

Weight function

The weight function value (*w*) is changed according to distance and nodes in the domain of effect, and then a smoothly approximate curved line is given. For the reason of this characteristic, approximated value is changed according to the movement of current along the distance. It is very important to select a weight function *w* in the MLSM. There is large range for selecting the weight function. The basic characteristics are described as follows: (i) number of weight function is positive; and (ii) weight function is defined as the function of distance between the two points (Lancaster and Salkauskas, 1981; Cinegoski et al., 1988; Belyschko et al., 1994; Singh, 2004).

Following Goto and Ogawa (1992) and Singh (2004), Equations 6 to 8 are multiplied by weight functions for elevations $w(r)_\eta$, and velocity components $w(r)_{u,v}$ where $r = \|\eta - \eta_i, u - u_i, v - v_j\|$ over the domain *V* as follows,

$$\int_V w(r)_\eta \frac{\delta\eta}{\delta t} dV + \int_V w(r)_\eta \frac{\delta}{\delta x}(hu) dV + \int_V w(r)_\eta \frac{\delta}{\delta x}(hv) dV = 0 \quad (16)$$

$$\int_V w(r)_u \frac{\delta u}{\delta t} dV + g \int_V w(r)_u \frac{\delta\eta}{\delta x} dV = 0 \quad (17)$$

$$\int_V w(r)_v \frac{\delta v}{\delta t} dV + g \int_V w(r)_v \frac{\delta v}{\delta y} dV = 0 \quad (18)$$

Tsunami water elevation derived from Equation 4, velocity components and their weighting functions are integrated in each three node triangular elements with the interpolation function $\phi_i^T(x)$ that is obtained from Equation 15.

RESULTS AND DISCUSSION

The multispectral QuickBird satellite data shows great turbulent flow along coastal water of Kalutara (Figure 4a). In fact, the tsunami wave is curved around the southern part of Sri Lanka and attacked the west coast and caused strong turbulent flow. This turbulent flow has spelled out the name of Allah in Arabic (Marghany and Suffian, 2005; Marghany and Mazlan, 2011). Figures 4b and c show the tsunami spectra that were extracted using 2-DFFT with kernel window size of 512 × 512 pixels and lines in two different areas in the QuickBird data (Figure 4a). Figures 4b and c show different patterns of tsunami wave spectra along the coastal water. Figure 4b depicts tsunami wave spectra direction of 150° is towards the coastline, while Figure 4c shows wave propagation is towards 70°. It is interesting to find the dominant wavelength is between 50 and 200 m. The changes of wave direction from area A to B are because of diffraction. According to Marghany and Suffian (2005) and Marghany and Mazlan (2011), the tsunami waves have diffracted around Sri-Lanka island and then moved perpendicular to the Kalutara coast and spread inland, causing widespread flooding. Figure 4a shows that the water drained back into the ocean and it built two barriers along Kalutara coastline. As successive tsunami passed along the large two barriers, the wave is then diffracted. Therefore, another barrier is blocked part of the wave and allow the rest to pass and generated large eddy with radius of 150 m behind the barrier. This indicates that the successive tsunami waves that hit the Kalutara coastline have changed the coastal zone morphology pattern (Marghany and Mazlan, 2011).

Figure 5 shows the 3-D wave run-up which is between 2 and 6 m wave height. The maximum wave height is shown across an eddy movement while the waves have spread inland was between 2 and 4 m height. Figure 5 shows 3-D dimensions for wave diffraction along Kalutara coastline. This indicates that turbulent water movement due to combination of wave diffraction, refraction and long-shore current movement between the two barriers.

(a)

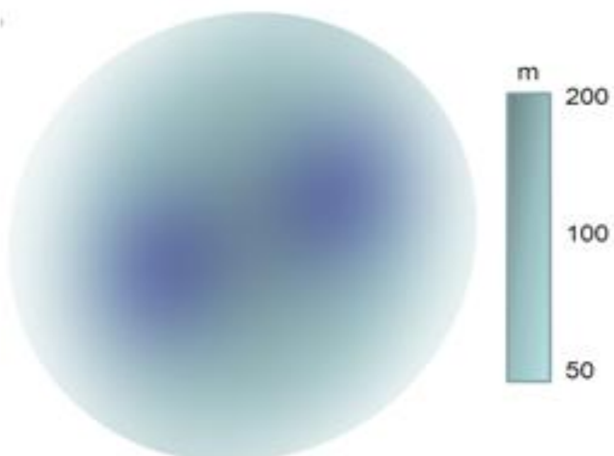

(b)

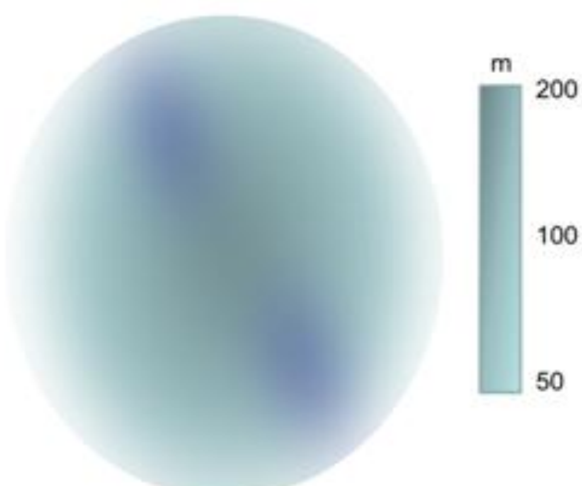

(c)

Figure 4. (a) Selected Kernel windows, (b) tsunami spectra at area A and (c) tsunami spectra at area B.

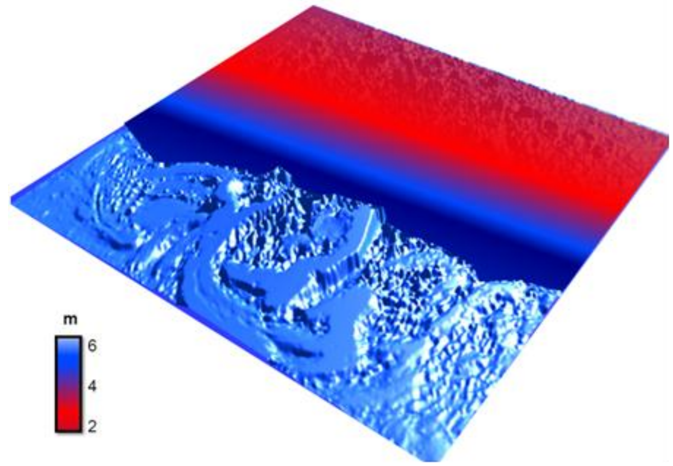

Figure 5. 3-D tsunami run-up pattern variation.

Taken together, these were able to cause a pattern which spell out, approximately the pattern of the Arabic word for Allah.

Clearly, EFGM algorithm is able to reconstruct 3-D visualization of tsunami the propagation and run-up in QuickBird satellite data. High resolution of 0.6 m is relieving EFGM algorithm to perform accurate visualization. In this regard, high resolution of QuickBird is able to capture afine information about tsunami morphology propagation (Figure 4a). Further, EFGM is able to track fine information regarding tsunami causing rough turbulent flow along the coastal water of Kalutara. EFGM based a mesh-less method, therefore, does not need a time-consuming mesh generation for modeling the computational domain of tsunami propagation in QuickBird satellite data. This confirms the study of Belyschko et al. (1994). Further, MLSM is used to acquire state value of arbitrary evaluation points in the domain For the EFGM. On other hand, the MLS method can be used in function approximation which reconstructs the continuous function from an arbitrary set of particles by calculating a weighted LS around the evaluation point. Consistent with Hiroshi et al. (1994), the MLS is precise than the grid-based numerical methods near irregular surfaces such as tsunami wave propagation. Finally, the weight function in MLS is flexible to track the changes of the different parameters in every three node triangular element with the integration of linear interpolation function. This confirms the studies of Lancaster and Salkauskas (1981), Cinegoski et al. (1988) Belyschko et al. (1994), Hiroshi et al. (1994), Singh (2004), Gedik et al. (2005) and Marghany and Mazlan (2011).

Conclusion

This work has demonstrated a new approach to simulate 3-D tsunami run-up in high resolution multispectral satellite data of QuickBird. In doing so, 2-DFFT algorithm is implemented to model tsunami wave spectra parameters of wavelength, wavenumber and direction. Then, EFGM based on mesh-less method used to solve the shallow water wave equations for wave spectra simulated from QuickBird data. In addition, moving least square method used to acquire state value of arbitrary evaluation points in the domain for EFGM. The study shows that the tsunami run-up height is ranged between 2 to 6 m. Consequently, it is easy to discriminate between a rough surface flow structures and smooth surface flow. In fact, the EFGM is considers as deterministic algorithms which are described by optimize triangulation only locally between two different points. In addition, the involving weight function in moving least square method is able to keep track of uncertainty and provide tool for representing spatially clustered gradient tsunami run-up points. Finally, EFGM can be used for 3-D tsunami run-up reconstruction from high resolution multispectrall satellite data of QuickBird.

REFERENCES

Belyschko T, Lu YY, Gu L (1994). Element-Free Galerkin method. Int. J. Num. Meth. Eng., 37: 229-256.

Cinegoski V, Miyamoto N, Yamashita H (1988). Element-Free Galerkin Method for Electromagnetic Field Computations. IEEE Trans. Magnet., 34: 3236-3239.

Gedik N, Irtem E, Kabdasli S (2005).Laboratory investigation on tsunami run-up. Ocean Eng., 32: 513-528.

Goto C, Ogawa Y (1992). Numerical Method of Tsunami Simulation with the Leap-frog Scheme. Department of Civil Engineering, Tohoku University. Translated for the TIME Project by N. Shuto, pp. 1-15.

Hiroshi O, Toshiro N, Genki Y (1994). Basic study on Element-Free Gelerkin Method (2nd report, application to two-dimensional potential problems). JSME Int. J., 95: 1825-1845.

Ibrahim SM, Nor ZW, Mohammed SAR, Kok FL (2009). Tsunami Hazard Evaluation using spatial tools for Kuala Muda, Kedah, Malaysia. Dis. Adv., 2(3): 5-14.

Joe F, Alexander B, Ranjit G, Janaka R, Chan SW (2012). A Journey through the Disaster with an Emphasis on Sri Lanka schulich.ucalgary.ca/civil/files/civil/IndianOceanTsunami.doc. pp. 1-30.

Kouchi K, Yamazaki F (2007). Characteristics of tsunami-affected areas in moderate-resolution satellite Images. IEEE Trans. Geos. Rem. Sens., 45(6): 1650 -1657.

Lancaster P, Salkauskas K (1981). Surfaces Generated by Moving Least Squares Methods. Math. Comput., 37: 141-158.

Lovholt F, Bungum H, Harbitz CB, Glimsal S, Lindholm CD, Pedersen G (2006). Earthquake related tsunami hazard along the western coast of Thailand. Nat. Haz. Earth Syst. Sci., 6(6): 979–997.

Marghany MM (2001). Opertional of Canny algorithm on SAR data for modeling shoreline change. Phot. Fern. Geo., 2: 93-102.

Marghany MM, Sufian M (2005). Simulation of The Successive Tsunami Waves along Kalatura Coastline from QuickBird-1 satellite. Asian J. Geo., 5(2): 13-25.

Nalbant S, Steacy S, Sieh K, Natawidjaja D, McCloskey J (2005). Seismology: Earthquake risk on the Sunda trench. Nat., 435(7043): 756-757.

Oo KS, Mehdiyev M, Samarakoon L (2005). Potential of satellite data in assessing coastal damage caused by South-Asia tsunami in December 2005 - A field survey report. Asian J. Geoinf., 5(2): 16-37.

Paris R, Lavigne F, Wassimer P, Sartohadi J (2007). Coastal sedimentation associated with the December 26, 2004 tsunami in

LhokNga, west Banda Aceh (Sumatra, Indonesia). Mar. Geol., pp. 93-106.

Populus J, Aristaghes C, Jonsson L, Augustin JM, Pouliquen E (1991). The use of SPOT data for wave analysis. J. Rem. Sen. Environ., 36: 55-65.

Sibuet JC, Rangin C, Le Pichon X, Singh S, Cattaneo A, Graindorge D, Klingelhoefer F, Lin JY, Malod J, Maury T, Schneider JL, Sultan N, Umber M, Yamaguchi H, the “Sumatra aftershocks” team, (2007). Great Sumatra-Andaman earthquake: Co-seismic and post-seismic motions in northern Sumatra. Earth Plan. Sci. Lett., 263(1-2): 88-103.

Singh IV (2004). Meshless EFG method in Three-Dimensional Heat Transfer Problems: A numerical Comparison, Cost and Errors Analysis. Num. Heat Transf., Part A., 46: 199-220.

Stein S, Okal EA (2005). Speed and size of the Sumatra earthquake. Nat., 434: 581-582.

Synolakis CE (1987). The runup of solitary waves. J. Flu. Mech., 185: 523-545.

USGS (2004). http://Earthquake.usgs.gov/eqinthenews.

Walter HF, Smith RS, Vasily V, Titov DA, Brian KA (2005). Satellite Altimeters Measure Tsunami. Oceanography, 18(2): 11-13.